Influence of Cations and Concentrations on the Morphology of Gypsum Crystals

Rep. Fac. Sci., Kagoshima Univ.
No. 31, 57~65, 1998.

Influence of Cations and Concentrations on the Morphology of Gypsum Crystals

Katsutoshi TOMITA[1], Aki KUWAHARA[1] and Motoharu KAWANO[2]

(Received August 21, 1998)

Keywords : Gypsum, Cation, Concentration, Morphology.

Abstract

Influences of various cations and concentrations of solutions on morphology changes of formed gypsum crystals in the solution were investigated.

Noting the influence of cations under equable concentration condition, the following evidences were clarified: (1) formed crystal sizes and aggregation conditions displayed dependence on cations, and (2) lengths of edges and angles of apexes also depicted dependency on cations. Noting the influence of concentrations, the following results were observed with increasing the concentrations: (1) crystal sizes decreased, (2) crystals having (111) plane increased, (3) crystal aggregates changed, and (4) plate-like crystals (including twin crystals) decreased.

Introduction

When crystals grow, the morphology is affected by the conditions of forming crystals. With regard to gypsum, several papers have been published (Kastner, 1970; Lindberg and Smith, 1973; Grattan-Bellow, 1975; Rodgers and Courtney, 1988; Rinaudo and Franchini-Angela, 1989). With regard to the morphology of gypsum, Rinaudo and Franchini-Angela (1989) reported that gypsum crystals form mechanical twins due to the existence of cations during the crystal growth. Gypsum is often found on the surfaces of wet volcanic ashes spewed from the Sakurajima volcano, and the shapes of the gypsum crystals assume many varieties. Tomita *et al.* (1985) showed the formation of different morphology of gypsum after wetting volcanic ashes from Sakurajima volcano. The morphology change is due to the different amount of SO_2 and/or H_2S and different cations contained in the volcanic ashes. The purpose of this paper is to estimate the kinds of cations attached on the surface of volcanic ashes by checking the shape of gypsum crystals formed on the surface of volcanic ashes.

Experimental Method

Each 10ml of solution containing chemical reagents of Na_2SO_4, $MgSO_4$, K_2SO_4, $FeSO_4$, and $Al_2(SO_4)_3$ were respectively mixed with 50ml of $CaCl_2$ solution, and left the mixed solution for a certain period of times after stirring. After the reaction took place, the reaction products were washed with distilled water several times, then dried in air. The dried samples were observed with scanning electron microscope. Some samples were investigated by X-ray diffraction method (XRD), differential thermal analyser (DTA), scanning electron microscope (SEM) and energy dispersive X-ray (EDX). For EDX, a HITACHI S-4000 FESEM scanning electron microscope equipped EDX facilities

[1] Department of Earth and Environmental Sciences, Faculty of Science, Kagoshima University, 1-21-35 Korimoto, Kagoshima
890-0065, Japan.

[2] Department of Environmental Sciences and Technology, Faculty of Agriculture, Kagoshima University, 1-21-24 Korimoto, Kagoshima 890-0065, Japan.

was used.

Results

Influence of kind of cations concentration

Experimental conditions and products for Na_2SO_4, $MgSO_4$, K_2SO_4, $FeSO_4$, and Al_2SO_4 are listed in Table 1, 2, 3, 4 and 5 respectively. Gypsum is always formed from the mixed solutions except from mixed solutions of low concentrations of Na_2SO_4 and $CaCl_2$, and of $MgSO_4$ and $CaCl_2$. X-ray diffraction patterns of the representative products are shown in

Table 1. Experimental conditions and products

Run No.	Na_2SO_4 (Mol)	$CaCl_2$ (Mol)	Reaction Time	Products
0505Na	0.5	0.5	30m	G
0510Na	1.0	0.5	30m	G
0515Na	1.5	0.5	30m	G
0520Na	2.0	0.5	30m	G
0525Na	2.5	0.5	30m	G
0530Na	3.0	0.5	30m	G
1005Na	0.5	1.0	30m	G
1010Na	1.0	1.0	30m	G
1015Na	1.5	1.0	30m	G
1020Na	2.0	1.0	30m	G
1025Na	2.5	1.0	30m	G
1030Na	3.0	1.0	30m	G
1505Na	0.5	1.5	30m	G
1510Na	1.0	1.5	30m	G
1515Na	1.5	1.5	30m	G
1520Na	2.0	1.5	30m	G
1525Na	2.5	1.5	30m	G
1530Na	3.0	1.5	30m	G
2005Na	0.5	2.0	30m	G
2010Na	1.0	2.0	30m	G
2015Na	1.5	2.0	30m	G
2020Na	2.0	2.0	30m	G
2025Na	2.5	2.0	30m	G
2030Na	3.0	2.0	30m	G
2505Na	0.5	2.5	30m	G
2510Na	1.0	2.5	30m	G
2515Na	1.5	2.5	30m	G
2520Na	2.0	2.5	30m	G
2525Na	2.5	2.5	30m	G
2530Na	3.0	2.5	30m	G
3005Na	0.5	3.0	30m	G
3010Na	1.0	3.0	30m	G
3015Na	1.5	3.0	30m	G
3020Na	2.0	3.0	30m	G
3025Na	2.5	3.0	30m	G
3030Na	3.0	3.0	30m	G
0101Na	0.1	0.1	43h	G
0202Na	0.2	0.2	43h	G
0303Na	0.3	0.3	43h	G
0404Na	0.4	0.4	43h	G
0505Na·43	0.5	0.5	43h	G
0520Na·43	2.0	0.5	43h	G
1005Na·43	0.5	1.0	43h	G
1020Na·43	2.0	1.0	43h	G
1505Na·43	0.5	1.5	43h	G
1520Na·43	2.0	2.0	43h	G

m:minutes, h:hours, G:gypsum

Table 2. Experimental conditions and products

Run No.	$MgSO_4$ (Mol)	$CaCl_2$ (Mol)	Reaction Time	Products
0505Mg	0.5	0.5	30m	G
0510Mg	1.0	0.5	30m	G
0515Mg	1.5	0.5	30m	G
0520Mg	2.0	0.5	30m	G
0525Mg	2.5	0.5	30m	G
0530Mg	3.0	0.5	30m	G
1005Mg	0.5	1.0	30m	G
1010Mg	1.0	1.0	30m	G
1015Mg	1.5	1.0	30m	G
1020Mg	2.0	1.0	30m	G
1025Mg	2.5	1.0	30m	G
1030Mg	3.0	1.0	30m	G
1505Mg	0.5	1.5	30m	G
1510Mg	1.0	1.5	30m	G
1515Mg	1.5	1.5	30m	G
1520Mg	2.0	1.5	30m	G
1525Mg	2.5	1.5	30m	G
1530Mg	3.0	1.5	30m	G
2005Mg	0.5	2.0	30m	G
2010Mg	1.0	2.0	30m	G
2015Mg	1.5	2.0	30m	G
2020Mg	2.0	2.0	30m	G
2025Mg	2.5	2.0	30m	G
2030Mg	3.0	2.0	30m	G
2505Mg	0.5	2.5	30m	G
2510Mg	1.0	2.5	30m	G
2515Mg	1.5	2.5	30m	G
2520Mg	2.0	2.5	30m	G
2525Mg	2.5	2.5	30m	G
2530Mg	3.0	2.5	30m	G
3005Mg	0.5	3.0	30m	G
3010Mg	1.0	3.0	30m	G
3015Mg	1.5	3.0	30m	G
3020Mg	2.0	3.0	30m	G
3025Mg	2.5	3.0	30m	G
3030Mg	3.0	3.0	30m	G
0101Mg	0.1	0.1	43h	G
0202Mg	0.2	0.2	43h	G
0303Mg	0.3	0.3	43h	G
0404Mg	0.4	0.4	43h	G
0505Mg·43	0.5	0.5	43h	G
0520Mg·43	2.0	0.5	43h	G
1005Mg·43	0.5	1.0	43h	G
1020Mg·43	2.0	1.0	43h	G
1505Mg·43	0.5	1.5	43h	G
1520Mg·43	2.0	2.0	43h	G

m:minutes, h:hours, G:gypsum

Table 3. Experimental conditions and products

Run No.	K_2SO_4 (Mol)	$CaCl_2$ (Mol)	Reaction Time	Products
0505K	0.5	0.5	30m	G
0510K	1.0	0.5	30m	G
1005K	0.5	1.0	30m	G
1010K	1.0	1.0	30m	G
1505K	0.5	1.5	30m	G
1510K	1.0	1.5	30m	G
2005K	0.5	2.0	30m	G
2010K	1.0	2.0	30m	G
2505K	0.5	2.5	30m	G
2510K	1.0	2.5	30m	G
3005K	0.5	3.0	30m	G
3010K	1.0	3.0	30m	G
0101K	0.1	0.1	43h	G
0202K	0.2	0.2	43h	G
0303K	0.3	0.3	43h	G
0404K	0.4	0.4	43h	G
0505K·43	0.5	0.5	43h	G
1005K·43	0.5	1.0	43h	G
1505K·43	0.5	1.5	43h	G

m:minutes, h:hours, G:gypsum

Table 4. Experimental conditions and products

Run No.	$FeSO_4$ (Mol)	$CaCl_2$ (Mol)	Reaction Time	Products
0505Fe	0.5	0.5	30m	G
0510Fe	1.0	0.5	30m	G
0515Fe	1.5	0.5	30m	G
0520Fe	2.0	0.5	30m	G
0525Fe	2.5	0.5	30m	G
0530Fe	3.0	0.5	30m	G
1005Fe	0.5	1.0	30m	G
1010Fe	1.0	1.0	30m	G
1015Fe	1.5	1.0	30m	G
1020Fe	2.0	1.0	30m	G
1025Fe	2.5	1.0	30m	G
1030Fe	3.0	1.0	30m	G
1505Fe	0.5	1.5	30m	G
1510Fe	1.0	1.5	30m	G
1515Fe	1.5	1.5	30m	G
1520Fe	2.0	1.5	30m	G
1525Fe	2.5	1.5	30m	G
1530Fe	3.0	1.5	30m	G
2005Fe	0.5	2.0	30m	G
2010Fe	1.0	2.0	30m	G
2015Fe	1.5	2.0	30m	G
2020Fe	2.0	2.0	30m	G
2025Fe	2.5	2.0	30m	G
2030Fe	3.0	2.0	30m	G
2505Fe	0.5	2.5	30m	G
2510Fe	1.0	2.5	30m	G
2515Fe	1.5	2.5	30m	G
2520Fe	2.0	2.5	30m	G
2525Fe	2.5	2.5	30m	G
2530Fe	3.0	2.5	30m	G
3005Fe	0.5	3.0	30m	G
3010Fe	1.0	3.0	30m	G
3015Fe	1.5	3.0	30m	G
3020Fe	2.0	3.0	30m	G
3025Fe	2.5	3.0	30m	G
3030Fe	3.0	3.0	30m	G
0101Fe	0.1	0.1	43h	G
0202Fe	0.2	0.2	43h	G
0303Fe	0.3	0.3	43h	G
0404Fe	0.4	0.4	43h	G
0505Fe·43	0.5	0.5	43h	G
0520Fe·43	2.0	0.5	43h	G
1005Fe·43	0.5	1.0	43h	G
1020Fe·43	2.0	1.0	43h	G
1505Fe·43	0.5	1.5	43h	G
1520Fe·43	2.0	2.0	43h	G

m:minutes, h:hours, G:gypsum

Table 5. Experimental conditions and products

Run No.	$Al_2(SO_4)_3$ (Mol)	$CaCl_2$ (Mol)	Reaction Time	Products
0505Al	0.5	0.5	30m	G
0510Al	1.0	0.5	30m	G
1005Al	0.5	1.0	30m	G
1010Al	1.0	1.0	30m	G
1505Al	0.5	1.5	30m	G
1510Al	1.0	1.5	30m	G
2005Al	0.5	2.0	30m	G
2010Al	1.0	2.0	30m	G
2505Al	0.5	2.5	30m	G
3005Al	0.5	3.0	30m	G
0101Al	0.1	0.1	43h	G
0202Al	0.2	0.2	43h	G
0303Al	0.3	0.3	43h	G
0404Al	0.4	0.4	43h	G
0505Al·43	0.5	0.5	43h	G
1005Al·43	0.5	1.0	43h	G
1505Al·43	0.5	1.5	43h	G

m:minutes, h:hours, G:gypsum

Table 6. X-ray powder diffraction data for gypsums

Sample No.	A		0510Na		0510Mg		2010K		0510Fe			
hkl	d(Å)	I/I_0	d(Å)	I/I_0	d(Å)	I/I_0	d(Å)	I/I_0	d(Å)	I/I_0	d(Å)	
020	7.56	100	7.56	100	7.56	100	7.56	100	7.56	100	7.56	100
$12\bar{1}$	4.27	50	4.27	50	4.27	67	4.27	86	4.27	18	4.27	88
031, 040	3.79	20	3.79	14	3.80	23	3.80	23	3.79	15	3.78	23
$11\bar{2}$	3.163	4	3.16	<1	3.164	3	3.176	5	3.164	<1	3.176	5
$14\bar{1}$	3.059	55	3.06	1	3.05	59	3.053	77	3.058	22	3.058	79
002	2.867	25	2.87	8	2.86	24	2.873	35	2.867	5	2.867	46
$21\bar{1}$	2.786	6	2.78	2	2.79	4	2.788	6	2.784	1	2.780	8
022, 051	2.679	28	2.68	6	2.68	17	2.683	10	2.683	4	2.680	33
150, $20\bar{2}$	2.591	4	2.59	2	2.59	4			2.592	2	2.590	6
060	2.530	<1	2.530	<1	2.530	<1			2.529	<1		
200	2.495	6	2.490	2	2.490	4	2.495	7	2.495	<1	2.490	11
$22\bar{2}$	2.450	4	2.450	2	2.450	3	2.455	6	2.449	1	2.440	6
141	2.400	4	2.400	1	2.400	2	2.401	3	2.398	<1	2.398	4
$15\bar{2}$	2.216	6	2.217	3	2.217	7	2.217	11	2.217	3	2.217	11
$24\bar{2}$	2.139	2	2.139	<1	2.141	2	2.141	2	2.141	<1	2.141	2
$12\bar{3}$	2.080	10	2.085	3	2.080	9	2.080	12	2.085	2	2.080	18
112, $25\bar{1}$	2.073	8	2.073	1	2.070	9	2.047	3	2.071	2	2.070	14
170	1.990	4	1.989	1	1.989	2	1.990	3	1.989	2	1.994	3
211	1.953	2	1.953	<1	1.953	1	1.957	2	1.953	<1	1.953	3
080, 062	1.898	16	1.899	4	1.897	8	1.899	12	1.899	4	1.899	12
$14\bar{3}$	1.879	10	1.881	2	1.879	6	1.879	8	1.879	2	1.877	9
$31\bar{2}$	1.864	4	1.866	<1	1.865	2			1.862	<1		
231	1.843	2										
$26\bar{2}$	1.812	10	1.811	3	1.811	7	1.812	9	1.811	3	1.811	10
$32\bar{1}$	1.796	4	1.797	1	1.797	3	1.801	4	1.799	<1	1.797	6
260	1.778	10	1.778	2	1.778	5	1.781	7	1.778	2	1.778	8
$25\bar{3}$	1.711	2					1.710	1	1.710	<1		
$32\bar{3}$	1.684	2	1,684	<1	1.682	<1	1.684	2	1.684	<1	1.684	3
$34\bar{1}$	1.664	4	1.664	1	1.664	2	1.665	3	1.664	<1	1.667	4
$16\bar{3}$	1.645	2	1.645	<1	1.645	1	1.646	2	1.645	<1		
$20\bar{4}$	1.621	6	1.621	2	1.621	5	1.622	6	1.621	2	1.621	8
$35\bar{2}$, 190	1.599	<1							1.600	<1		
$22\bar{4}$	1.584	2	1.585	<1	1.583	1	1.586	3	1.585	<1	1.583	3
$28\bar{2}$	1.532	2	1.532	<1	1.532	<1	1.534	2	1.533	<1	1.533	2
a(Å)	5.68		5.67		5.67		5.68		5.61		5.61	
b(Å)	15.18		15.19		15.18		15.20		15.27		15.20	
c(Å)	6.51		6.53		6.52		6.52		6.52		6.52	
β	118°38′		118°48′		118°47′		118°68′		117°85′		118°49′	

A:ASTM card No.6-46.

Fig.1, and XRD data are listed in Table 6 together with their lattice constants. XRD data and lattice constants of these samples were observed to be not so different from each other.

Differential thermal analysis curves of these samples were almost the same. Five representative curves are shown in Fig. 2. The curves show a double low-temperature endothermic peak, corresponding to loss of water in two stages (i.e. loss of 1½ molecules to give $CaSO_4 \cdot ½$, and then dehydration to anhydrite).

Observations gleaned from the scanning electron microscope, showed that morphological changes of the formed crystals under different solutions

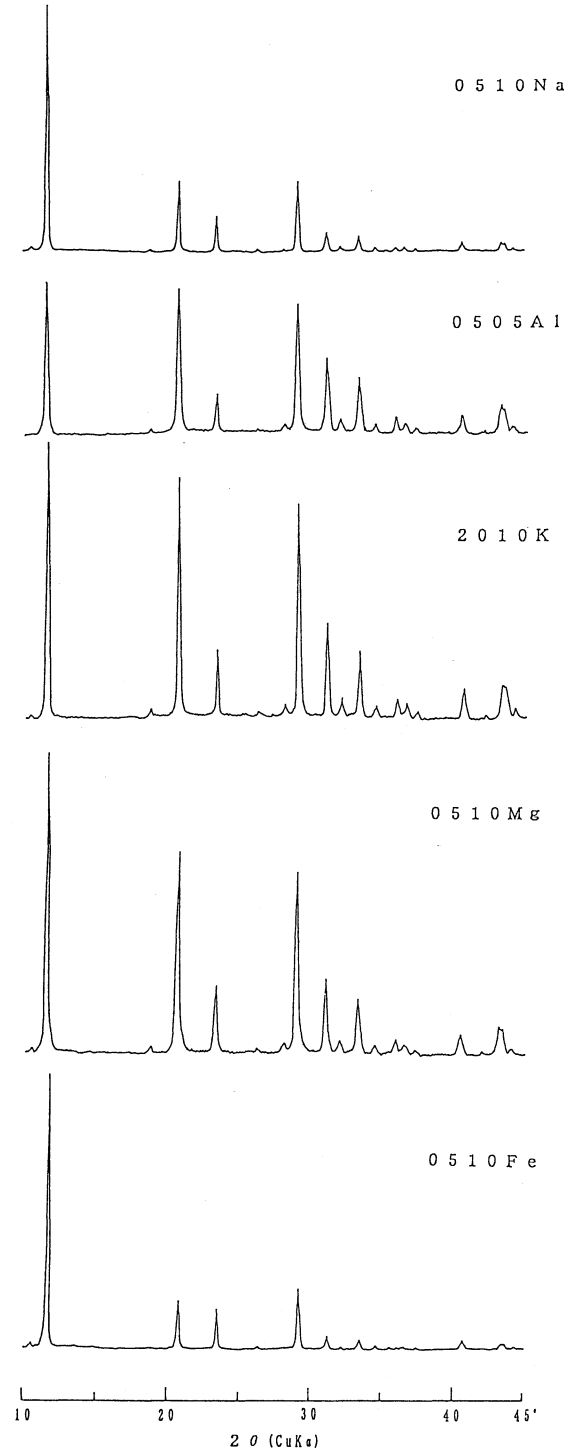

Fig. 1. X-ray diffraction patterns of formed gypsums under different conditions. 0510Na : 30 minutes reaction product from the solution of 0.5M Na_2SO_4 + 0.5M $CaCl_2$; 0505Al : 30 minutes reaction product from the solution of 0.5M $Al_2(SO_4)_3$ + 0.5M $CaCl_2$; 2010K : 30 minutes reaction product from the solution of 1M K_2SO_4 + 2M $CaCl_2$; 0510Mg : 30 minutes reaction product from the solution of 1M $MgSO_4$ + 0.5M $CaCl_2$; 0510Fe : 30 minutes reaction product from the solution of 1M $FeSO_4$ + 0.5M $CaCl_2$.

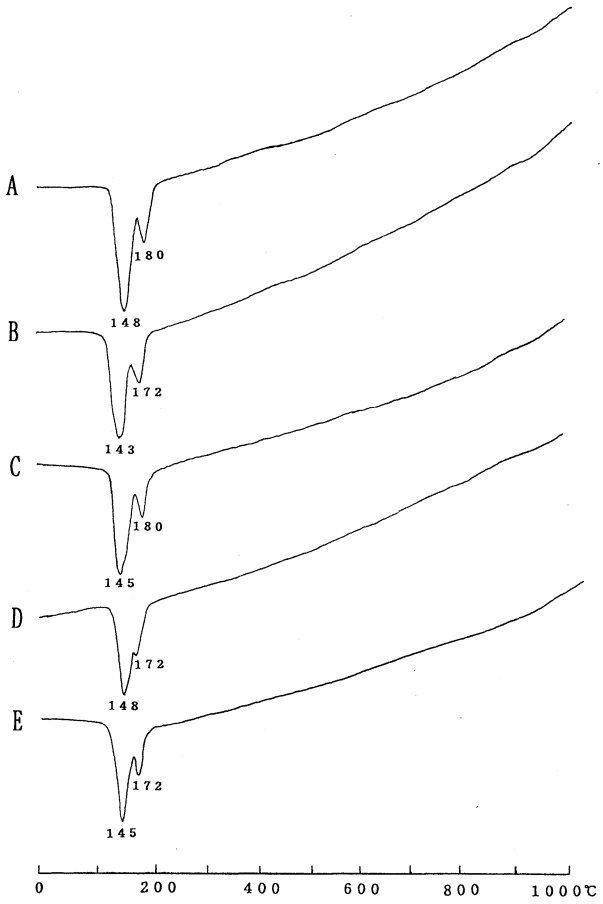

Fig. 2. Differential thermal analysis curves of the formed gypsums.
A : Sample No. : 1015Fe ; B : Sample No. : 1015Na ; C : Sample No : 1015Mg ; D : Sample No. : 1015K ; E : Sample No. : 1015Al.

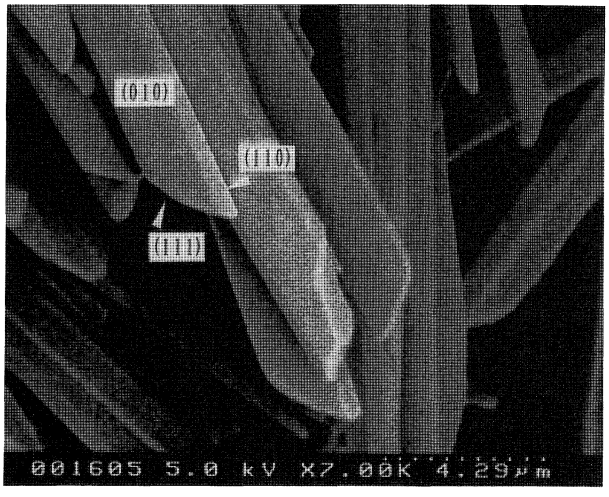

Fig. 3. Scanning electron micrograph of a formed gypsum.

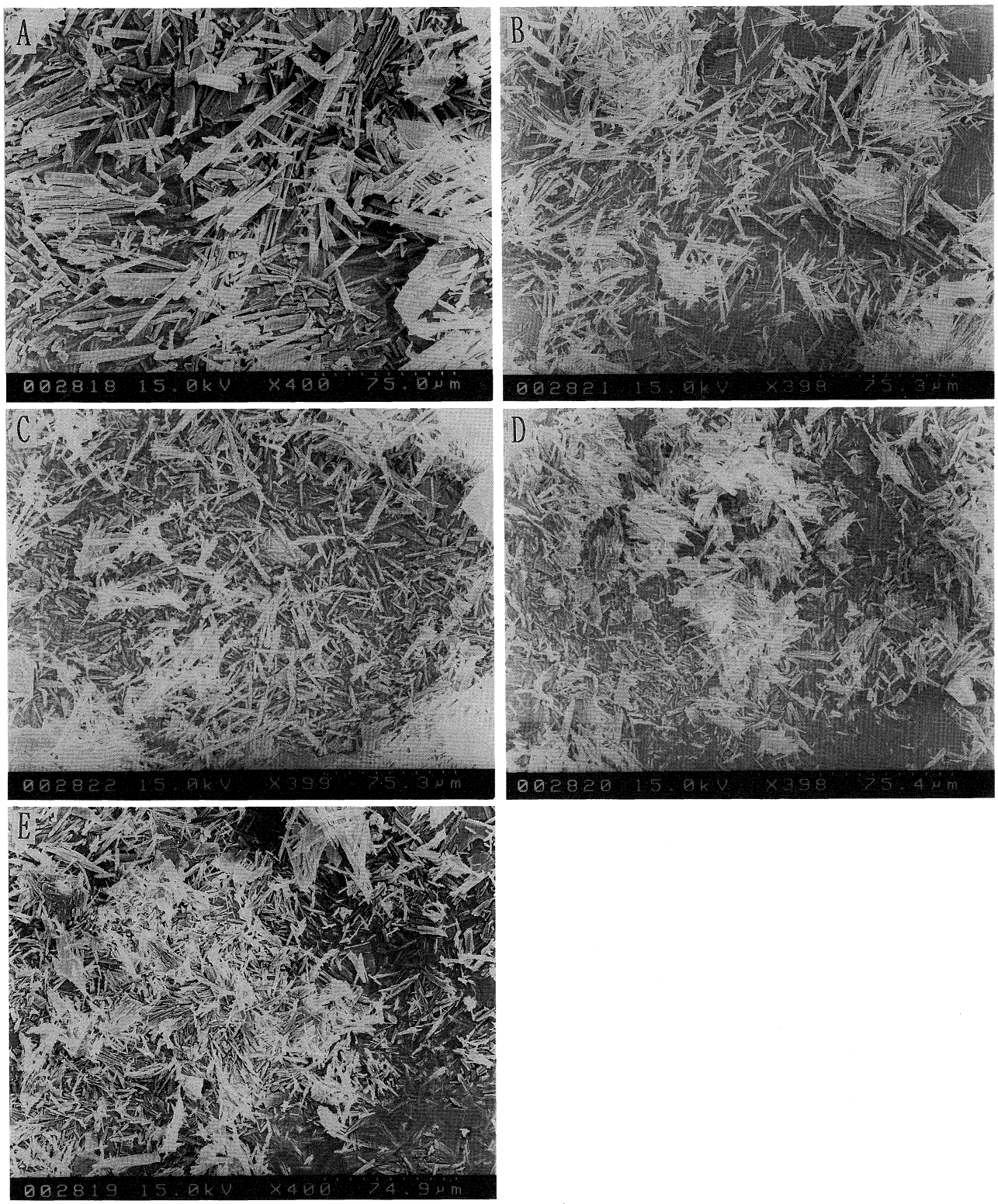

Fig. 4. Scanning electron micrographs of the formed gypsums. A : Sample No. : 1015Fe ; B : Sample No. : 1015Na ; C:Sample No : 1015Mg ; D : Sample No. : 1015K ; E : Sample No. : 1015Al.

containing different cations were not so essentially different. The (010) plane of every crystals was clearly observed and its size appeared large (Fig. 3). Planes (110) and (111) were a bit different from each other. Products from mixed solution of Na_2SO_4 and $CaCl_2$, and of $MgSO_4$ and $CaCl_2$, showed elongated thin plates, whereas crystals formed from mixtures of $MgSO_4$ and $CaCl_2$, and $Al_2(SO_4)_3$, showed thick elongated plates. Under the same concentrations (1M of $CaCl_2$ and 1M of added solution), crystals formed from mixed solutions such as $MgSO_4$ and $CaCl_2$, $FeSO_4$ and $CaCl_2$, and $Al_2(SO_4)_3$ and $CaCl_2$, showed a long large (111) plane, while crystals formed from solutions of K_2SO_4 and $CaCl_2$ also showed a long large (311) plane. Crystals formed from solutions of Na_2SO_4 and $CaCl_2$ exhibited a long large (211) plane besides (111) plane.

The crystal length is also shown to be substantially influenced by the concentration of the solution. Under unvarying concentration of solutions (0.5M of $CaCl_2$ and 0.5M of added solutions), crystals formed from a mixed solution of Na_2SO_4 and $CaCl_2$ showed a long (411) plane, and those from a mixed solution of $MgSO_2$ and $CaCl_2$ defined a long (211) plane. Crystals developed from a mixed solution of K_2SO_4 and $CaCl_2$ depicted a long (111) plane, while those from a mixed solution of $Al_2(SO_4)_3$ and $CaCl_2$ typified a long (511) plane. Under high concentrations of the solutions, sizes of the formed crystals are a bit illustrated slight dissimilarity from each other. Scanning electron micrographs of crystals formed under the same conditions are shown in Fig. 4. Crystal size and mode of aggregation were apparently influenced by the existing cations. Crystal size seemed to be larger when Fe^{2+} exists in the solution as compared with other cations.

Influence of concentration

In this paper concentration means the concentration of mixed solution. Crystals formed under low concentration of any solutions showed platy forms having cracks on the surface, and also showed twins (Fig. 5) and flower-like aggregates (Fig. 6). Consonant to the increase of concentration, aggregates of needle crystals were formed (Fig. 7A). Under the

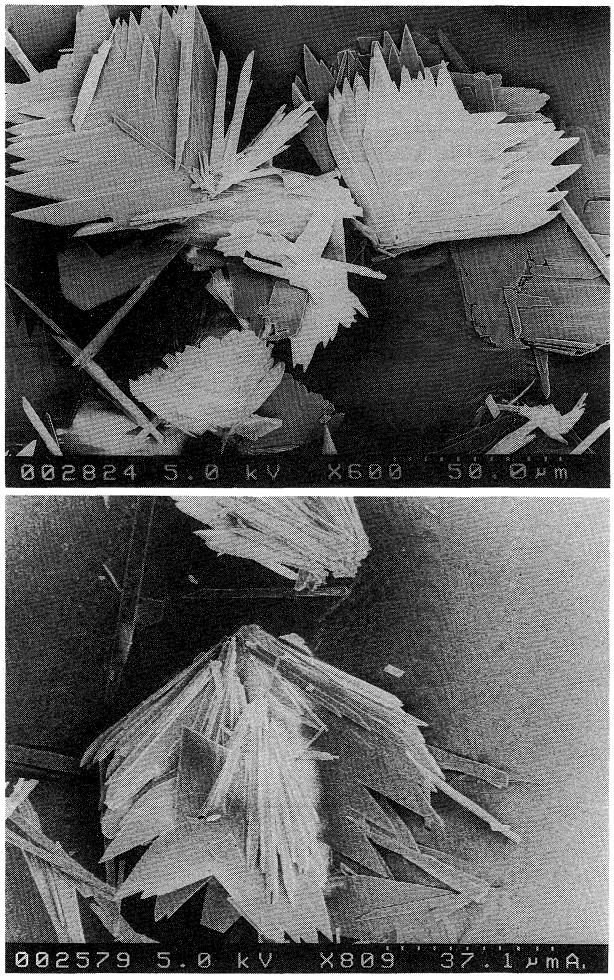

Fig. 5. Scanning electron micrographs showing platy crystals and twins.

Fig. 6. Scanning electron micrograph showing flower-like crystal.

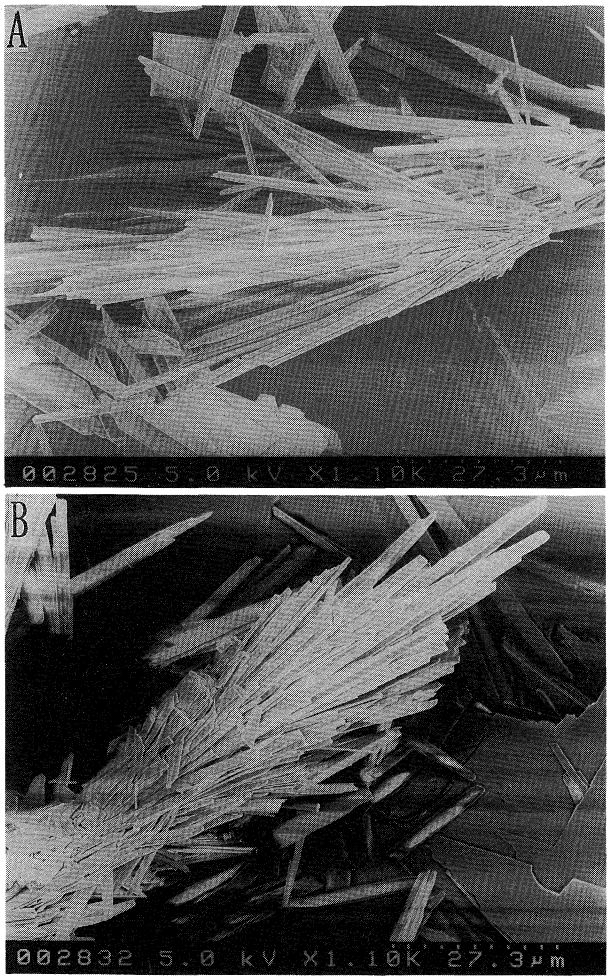

Fig. 7. Scanning electron micrographs showing aggregates of twin crystals (A) and leaves of Japanese cedars (B).

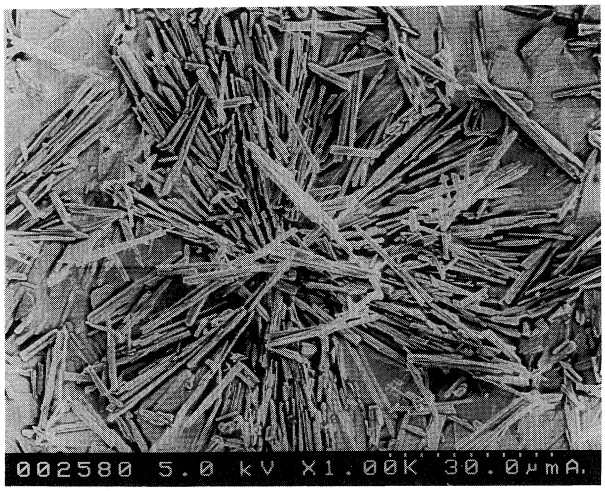

Fig. 8. Scanning electron micrograph showing stick-like crystals.

more concentrated condition, aggregates of short needle-like crystal resembling leaves of Japanese cedars were formed (Fig. 7B). Under higher concentrations, platy crystals were not observed and stick-like crystals were formed (Fig. 8).

Conclusion and Discussion

Based on the influence of cations under equal concentration condition, the following evidences were clarified. Formed crystal sizes and aggregation conditions displayed significant dependence on cations, and under the existence of Fe^{2+}, formed crystal sizes were apparently larger. Lengths of edges and planes and angles of apexes also showed strong dependency on cations. Under low concentration of solution, growth of plane (511) was remarkable with the existence of Al^{3+}. In the case of Na^{+} that of plane (411) was prominent, while for Mg^{2+} that of plane (211) was distinctive, and for K^{+} that of plane (311) was well-defined.

Regarding the influence of concentrations, results revealed that under low concentrations, many plate-like crystals and twin crystals were formed. Conversely, the increase in concentration brought diagnostic changes on crystal aggregation. The plate-like crystals and twin crystals notably decreased. The crystal sizes also recognizably decreased. Under high concentrations, radiated stick-like crystals were dominant.

Under low concentrations, crystals were observed to have formed slowly, and the resulting crystals were large, whereas, under high concentrations, crystal growth rate is high, and consequently crystals formed were many but comparatively smaller. Under low concentrations, vent crystals were also observed. It is said that vent crystals are due to the impurities included in the crystals. The authors analysed such impurities of the formed gypsum crystals using EDX, and it was confirmed that impurities were not included in the crystals. Twin crystals and platy crystals were observed only in low concentrations. Why those crystals formed under low concentration conditions are not yet fully understood, and therefore further study is still necessary.

Acknowledgments

The authors are indebted to T. Kakoi of Kagoshima University for his technical assistance.

References

Bottrell, S. H. (1991) Sulphur isotope evidence for the origin of cave evaporates in Ogofy Daren Cilau, south Wales. Miner. Mag., **55**, 209-210.

Grattan-Bellow, P. E. (1975) Effects of preferred orientation on X-ray diffraction patterns of gypsum. Amer. Miner., **60**, 1127-1129.

LindBerg, J. D. and Smith, M. S. (1973) Reflectance spectra of gypsum sand from the white sands national monument and basalt from a nearby lava flow. Amer. Miner., **58**, 1062-1064.

Kastner, M. (1970) An inclusion hourglass pattern in synthetic gypsum. Amer. Miner., **55**, 2128-2130.

Rinaudo, C. and Franchini-Angela, M. (1989) Curvature of gypsum crystals induced by growth in the presence of impurities. Miner. Mag., **53**, 479-482.

Rodgers, K. A. and Courtney, S. F. (1988) Mineral records from Funafuti, Tuvalu: gypsum, brucite, ettringite. Miner. Mag., **52**, 411-414.

Tomita, K., Kanai, T., Kobayashi, T. and Oba, N. (1985) Accretionary lapilli formed by the eruption of Sakurajima volcano. J. Japan. Assoc. Miner. Pet. Econ. Geol., **80**, 49-54.